



WPI

A QCM-D Analysis of Nanosilver Interactions with Supported Lipid Bilayers (SLBs) in the Presence of Natural Organic Matter (NOM)

A Major Qualifying Project (MQP) Submitted to the Faculty of

WORCESTER POLYTECHNIC INSTITUTE

In partial fulfillment of the Requirements for the Degree of Bachelor of Science (B.S.)
In
Chemical Engineering (CM)

Submitted by:

Charles E. DeWitt

Katie Hurlock

Ian M. Smith

Kara P. Upton

Date: April 26, 2018

Submitted to:

Professor Terri Camesano, Ph.D.

This report represents the work of four WPI undergraduate students submitted to the faculty as evidence of completion of a degree requirement. WPI routinely publishes these reports on its website without editorial or peer review. For more information about the projects program at WPI, please see: <http://www.wpi.edu/Academics/Projects>.

Abstract

The development of nanotechnology across a variety of industries has resulted in an influx of engineered nanoparticles (ENPs) to the environment where their toxicity to biological systems remains largely unknown. In aqueous solutions, natural organic matter (NOM)—a supramolecular complex consisting of decomposed remains—stabilizes ENPs and intensifies their toxicological effects. We investigated the size-dependence of silver nanoparticle interactions with L- α -phosphatidylcholine (PC) supported lipid bilayers (SLBs) when equilibrated with 20 mg/L of four NOM analogs: Suwannee River Humic Acid Standard II (SRHA) and Suwannee River Fulvic Acid Standard II (SRFA), two low-molecular weight samples, and Elliott Soil Humic Acid Standard IV (ESHA) and Leonardite Humic Acid Standard (LHAS), two high-molecular weight samples. We isolated the effective interaction of 20 nm, 40 nm, and 50 nm silver nanoparticles at a concentration of 1×10^{10} NP/mL using quartz crystal microbalance with dissipation monitoring (QCM-D) and Voigt-Kelvin viscoelastic modeling. QCM-D data was supplemented by dynamic light scattering (DLS) measurements of nanosilver-NOM aggregation in solution. The investigation aimed to develop a mechanistic model for nanosilver interactions with SLBs and contribute to a better understanding of ENP behavior in aquatic ecosystems. The basic research aims to inform regulators of the toxicological risk associated with the accumulation of ENPs in the environment.

Table of Contents

Abstract	2
1. Introduction	4
2. Background	5
2.1. Silver Nanoparticles	5
2.2. Supported Lipid Bilayers	6
2.3. Quartz Crystal Microbalance with Dissipation Monitoring (QCM-D)	8
2.4. Data Collection with the Q-Sense Analyzer and Flow Module	9
2.5. Replication of Environmental Conditions: Humic Substances as NOM Analogs	11
2.6. Natural Organic Matter (NOM)	11
2.7. Humic Substances as NOM Replicates	11
2.8. Hypothesis	12
3. Methods and Materials	13
3.1. Silver Nanoparticles	13
3.2. Humic Substances	13
3.3. Vesicle Preparation	13
3.4. Quartz Crystal Microbalance with Dissipation (QCM-D) Monitoring for Nanoparticle Interaction with Supported Lipid Bilayers	14
4. Results	15
4.1. Characterization of Humic Substances	15
4.2. SLB Formation by QCM-D	15
4.3. Interaction of SLB with NPs in the Presence of Humic Substances	16
5. Discussion	22
5.1. SRHA Induced the Only Significant SLB Disruption	22
5.2. Humic Substance Molecular Weight Did Not Affect Disruption Mechanics	22
5.3. Recommendations for Future QCM-D Analysis of NP-Induced SLB Disruption in the Presence of NOM	22
6. Conclusion	24
References	25

1. Introduction

The development of nanotechnology across a variety of industries has resulted in an influx of nanoparticles in the environment. Engineered nanoparticles (ENPs)—due to their small size (less than 100 nm) relative to cells and their large surface area to volume ratio (which increases their susceptibility to chemical interactions)—pose biological risks to the environment. However research on their toxicity remains largely undeveloped (Hwang, 2017). Nanosilver is particularly intriguing due to its popularity in commercial products such as odor-eliminating antibacterial agents. Further, the United States remains behind Europe in the regulation of nanotechnology in industry as safe size and concentration thresholds have yet to be established (Heerklotz, 2007). The goals of this project are to:

1. Establish concentration thresholds for observable supported lipid bilayer (SLB) destabilization as preliminary toxicity thresholds for nanoparticle regulation in the environment.
2. Characterize nanoparticle-natural organic matter (NOM) complexes in solution to understand the properties that make them toxic in the environment.

We used quartz crystal microbalance with dissipation monitoring (QCM-D) to form model cell membranes in the form of SLBs. These SLBs formed via vesicle adsorption and rupture on the quartz crystal. The vesicles were prepared through a series of freeze-thaw cycles and ice-bath sonication. The lipid constituents of the SLBs were determined by the biological targets of interest in the environment, in this case a simple PC bilayer generally reflective of microbes (Bailey et. al, 2015).

Through these studies, we aimed to explore the effect of silver nanoparticle size on SLB interactions independent of differences in concentration. We studied the aggregation of nanoparticle complexes with natural organic matter isolates using dynamic light scattering. We used humic substances as analogs for NOM found in water, sediment, and soil. Light scattering was used to interpret solution properties of humic substances, such as size, pH dependency, and salt dependency. We looked at a range of molecular weights for the NOM.

The Major Qualifying Project (MQP) presented herein is a progression from previous QCM-D studies focusing on the effect of concentration on the interactions of functionalized gold nanoparticles with model cell membranes (Kamaloo et. al, 2015); the size dependence of gold nanoparticle behavior with a supported lipid bilayer has also been studied by Professor Camesano's research group (Bailey et. al, 2015). Development of a mechanistic model for nanosilver interactions with SLBs would contribute to a better understanding of NP toxicity in the presence of NOM and inform regulators of the health risks associated with the accumulation of NPs in the environment.

2. Background

This investigation aims to establish concentration thresholds for observable supported lipid bilayer (SLB) destabilization in the presence of silver nanoparticle complexes. In this section, we present a literature review of silver nanoparticle transport and bioavailability in the environment. Further, we delineate the principles behind quartz crystal microbalance with dissipation monitoring (QCM-D) technology that enable the modeling of agglomerate interaction with model cell membranes. Finally, we consider the chemical transformation of nanoparticles in the environment that influence their interaction with biological systems.

2.1. Silver Nanoparticles

Silver nanoparticles are simply small pieces of silver ranging from 1 nm to 100 nm. They have a large volume to surface area ratio, usually leading to the outer surface being composed mostly of silver oxide. Many characteristics can affect the functionality of these particles, including shape, composition, and microstructure. Currently, there is a wide use of silver nanoparticles in industry. While they serve to be useful in a variety of ways, their impact on the environment is poorly understood. Research on their impact to plants, animals, and humans are minimal. Healthy concentration limits are not defined, and these particles continue to find their way into the environment with uncharacterized toxicity results (Welles, 2010).

The unique properties of silver nanoparticles make them attractive for many industries. They have unique optical, electronic, and chemical properties. This is due to their ability to effectively interact with photons by virtue of the surface plasmon resonance (Welles, 2010). These qualities prove to be effective to build from for diverse photonic devices. They also show antibacterial properties, with considerable amounts of bioactivity, making them of interest to both agricultural and medical fields. They have desirable physical and chemical bulk properties, but prove to be unreliable with their surface properties. They are believed to be integral in the biological function of biomolecules (Welles, 2010), but research has yet to determine specifics on exactly how these molecules disrupt cell membranes.

Recent research has been on increasing silver nanoparticles use in therapeutic delivery by creating a functionalized surface on the nanoparticle with antibodies/peptides/small molecules being used as a target (Welles, 2010). Through the studies, they have found that surfaces can be altered in a variety of ways. One common way is to use phospholipid derivatives with disulfide groups. They are very stable, and have a very good biocompatibility. They have a promising future in this industry, but not until dangerous concentrations and alternative effects are researched.

Commercially, silver nanoparticles are also popular. Silver is known to reduce odor. Many clothing manufacturers utilize this quality in production, specifically for socks. After their clothing is bought, around 50% of the nanoparticles in the product are estimated to escape into the environment after only the first few washes (Beyond Pesticides 2017). The particles travel from the wash to the sewers, and are commonly mixed with natural organic matter as they travel to bodies of water. They have been found in multiple samples of sewage sludge and water treatment plants (Beyond Pesticides 2017). They pose a threat to wastewater treatment plants because they inhibit growth of microbes that are essential to treatment. When nanoparticles find their way to a natural body of water, a portion of the nanosilver that finds its way into the environment associates with other ions and materials in the natural sediments. The rest of the

nanoparticles remain in the water, and have the opportunity to be ingested by the aquatic life. Additionally, they can enter the human body through air or liquid suspensions, and in concentrations ranging from 1-10 ppm could potentially affect human health (Welles, 2010).

When silver nanoparticles end up in soil, they can have effects on the plants that grow there. One experiment, completed by scientists Marty Mulvihill and Wendy Hessler, silver nanoparticles were dosed in soil with up to 18 parts per million. The amount of silver nanoparticles in the plants growing in that area were observed. These high silver nanoparticle concentrations remained high in plants located away from the water, while areas closer to the water had levels between 1 and 7 parts per million. Only plants that began growing after the soil was dosed were examined, indicating that plants absorbed the nanosilver from the soil. The silver nanoparticles that ended up in the water had alternative results. Over 50% of the nanoparticles were found to react with sulfur to form silver sulfide, about 30% bonded with organic matter, and the other 20% were left unreacted in the water (Mulvihill, 2016). It is important to note these reactions while investigating toxicity in natural, realistic setting. Nanosilver that reacts with other compounds becomes less toxic. Their function and structure are altered. Despite this, particles were still found in insects and fish. Fish passed silver on to their embryos, which could possibly affect the health and population of fish (Mulvihill, 2016).

Silver nanoparticles are currently the most commonly used nanoparticles due to their wide use in industry and their promising chemical properties can lead to predictions that they will grow even more in the recent future in popularity. It is integral that risks are investigated for these particles, especially in realistic settings (Urquhart, 2014).

2.2. Supported Lipid Bilayers

Molecular studies regarding cell surface interactions have been of interest to scientific minds for many years. Understanding the process by which biological and cellular information is transferred from one cell to another can be very effective in understanding how a certain cell functions (Castellana, 2006). Understanding how certain cells function could lead to advancements in biological technology as well as advancements in medical applications (Castellana, 2006). For our report, we will be studying the interactions of how silver nanoparticles interact with a cell membrane or a substitute that mimics the functions of a cell membrane. Our team will be using supported lipid bilayers, SLB, to mimic the functions of a cell membrane in order to study the surface disruptions that silver nanoparticles have with the surface of a cell.

The surface of a cell is referred to as a cell membrane, which is a semi-permeable barrier that surrounds the cell in order to protect the organelles of the cell (Bailey, 2017). Cell membranes are comprised of two different components, those being proteins and lipids (Bailey, 2017). Lipids contain a hydrophilic head that contains phosphate and a hydrophobic tail that is comprised of two hydrocarbon chains (Cooper, 2000). These lipids, also known as phospholipids, spontaneously create a lipid bilayer because of the properties of their heads and tails when introduced to aqueous solutions. Two pairs of the hydrophobic hydrocarbon chains that make up the lipid tail face inward toward one another to avoid being exposed to aqueous solutions (Richter, 2006). In order to ensure that the hydrocarbon chains are not exposed to water the polar head of the lipid faces toward the aqueous solutions and the hydrophilic heads bind with one another to create a barrier or membrane (Ritcher, 2006). The lipid heads face outside the cell as well as inside the cell, because of this formation the phospholipid bilayer forms.

(Cooper, 2000). Figure 1 below demonstrates the interaction of two lipid layers binding with one another to create a lipid bilayer that surrounds the cell.

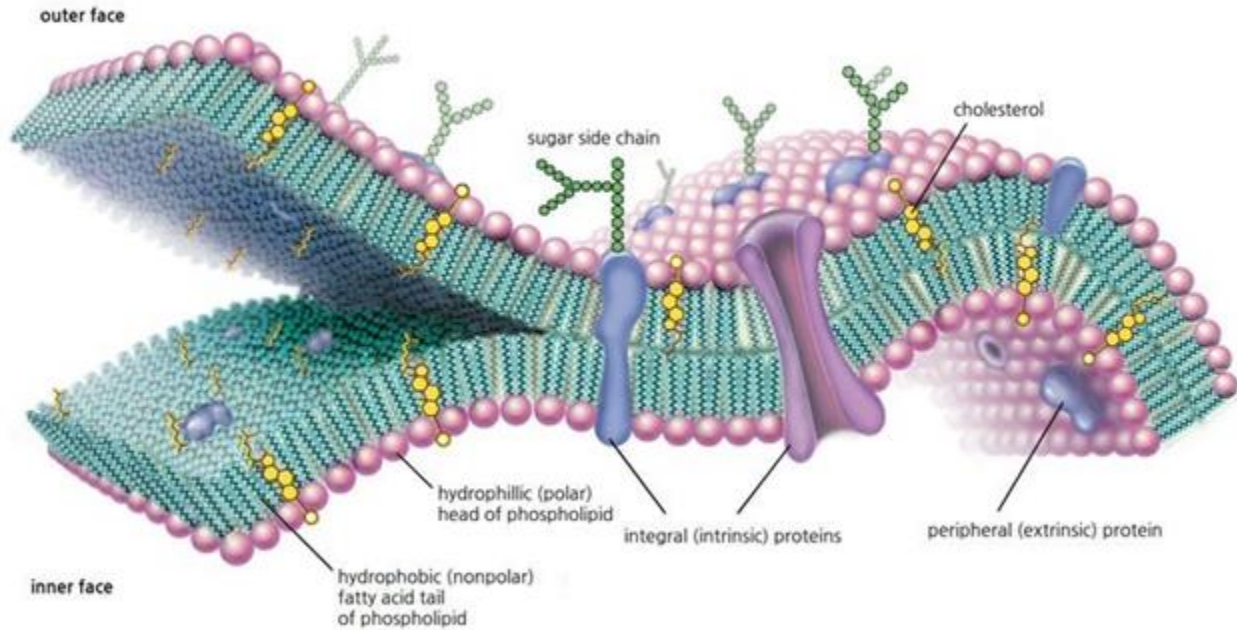


Figure 1. An illustration demonstrating a lipid bilayer (Bailey).

The other main component that makes up the cell membrane are the proteins. There are two types of proteins that are connecting with the cell membrane. Those proteins are peripheral and integral membrane proteins (Bailey, 2017). Peripheral membrane proteins are proteins that are attached to the exterior of the cell membrane due to interaction with integral proteins that are present at the cell membrane surface (Bailey, 2017). Integral membrane proteins are proteins that are embedded into the cell membrane (Ritcher, 2006). Both types of membrane proteins have many functions that assist in day to day operations within the cell. These proteins can be used to create other types of proteins that are required for organelle operation, to communicate what types of molecules can come in and out of the cell membrane, and can be used to transport molecules throughout the cell (Ritcher, 2006). Both lipids and proteins are essential to understanding cell surface interactions. Models of cell membranes have been created and study to investigate cell surface interactions. Two cell membrane models that our team plans to use to understand silver nanoparticle cell surface disruptions are supported lipid bilayers and vesicles as these models share similar functions to the cell membrane.

Supported lipid bilayers (SLBs) and vesicles are very good models for the cell membrane as they perform most of the same functions as the cell membrane does. SLBs perform many of the same intermembrane functions which include protein transportation, creation, and adsorption (Ritcher, 2006). Vesicles are simply lipid bilayers that are very prominent within the cell. Where SLBs have protein functions that are identical to the cell membrane, vesicles generally don't contain as much protein complexity. Both these bilayer models are very useful when

understanding surface interaction because they can both be synthetically and naturally produced. SLBs can be formed a number of ways, but one method of SLB formation is through vesicle fusion to create SLBs. SLBs and vesicles both contain phospholipid bilayers, which allows vesicles to open their membrane to fuse into a more supported lipid bilayer (Castellana 2006). It is important to have a stable SLB for testing to truly understand how the porous lipid bilayer would be affected by silver nanoparticle interaction. In order to understand the effect that silver nanoparticles would have on a SLB there would need to be a way to quantify the size of the bilayer before disruption. Quartz crystal microbalance with dissipation monitoring (QCM-D) is a way to quantify the effects that silver nanoparticles have on the SLBs as well as vesicles.

2.3. Quartz Crystal Microbalance with Dissipation Monitoring (QCM-D)

The main technique that we will be using for the supported lipid bilayers is Quartz Crystal Microbalance with Dissipation monitoring (QCM-D). The QCM-D is a nanoscale technique balance that analyzes surface phenomena such as reactions, interactions, and thin film formation (“Q-Sense Technologies”). The equipment is set up with a thin quartz disc lodged between two electrodes. Because of the set up with the thin quartz disc placed between the two electrodes and the fast oscillations from alternating voltages, the QCM-D is a very sensitive balance. The frequency and energy dissipation results of the oscillating sensor add to this sensitivity (“Q-Sense Technologies”). By differing the voltages, oscillations can be created and recorded. The results that are retrieved from the QCM-D are much faster and more accurate than other monitoring systems (“Q-Sense Technologies”).

With this piece of equipment, the sensor used to collect the data is called a QSensor. They are developed and produced to provide stable, reliable, and reproducible results. With each QSensor, there is a top coating material, and for this project we will be using the QSensors with a silicon dioxide top coating. Further information on the sensor’s description, surface roughness, usage, chemical compatibility, and more is shown in Figure 2 below.

Description	QSX 303 SiO ₂
Top Coating Material	Silicon dioxide (SiO ₂)
Surface Roughness	< 1 nm RMS
Maximum Temperature	150 degC
Chemical Compatibility	Do not expose to strong bases. There is no guarantee that the coating will be stable under all experimental conditions

Figure 2. A more in-depth description of the QSensor QSX 303 SiO₂ that will be used for this project adapted from Q-Sense Technologies.

As Figure 2 suggests, each QSensor QSX 303 SiO₂ has an intended use for one-time only. With each of these uses, a QSense Analyzer takes the data, and flow modules can be used as an accessory with a separate flow module for each sensor. The QSense Analyzer is used for its fast sample processing at a high quality. It is a 4-channel system which allows a high throughput

with an evaluation of multiple parameters at once, such as mass, thickness, and concentrations (“Q-Sense Technologies”). By analyzing all of that data at once, it is easy to compare multiple parameters from the same trial. The flow modules used in this sensor are easily removable, which adds flexibility and ease with the cleaning process for each trial. These flow modules have an aluminum shell with titanium liquid contacting surfaces and a sealing of Viton® for the O-rings (“Q-Sense Technologies”). Viton is a fluoroelastomer that is typically used for O-rings and is known for providing peak performance and resistance (“Minimize Downtime and Maximize Seal Performance with Viton™ Fluoroelastomers”). The flow module has a specified volume above the sensor of $40\mu\text{L}$, and the minimum sample volume is $250\mu\text{L}$. In addition, there is a loop in the flow module that stabilizes temperature so that the signals from the instrument are controlled (“Q-Sense Technologies”).

2.4. Data Collection with the Q-Sense Analyzer and Flow Module

The data that is collected from a QSense Analyzer with the flow module will represent something similar to Figure 3. Figure 3 outlines the frequency and dissipation changes as a function of time. In the figure below, the blue shows the frequency changes and the orange shows the dissipation changes. Phase 1 of the graph shows the binding of a small globular molecule, as shown on the bottom of the figure. At this point, there is a moderate frequency change (Δf) which is an indication of mass change. At the same time there is a low dissipation change (ΔD), indicating the rigidity of the film. In phase 2 of the graph, the large elongated molecule is binding to the surface. At this point there is a large change in frequency, due to the added mass, and a large change in dissipation, indicating a soft film. Finally, in the third phase of the graph, this is when the rinsing occurs with the regenerating buffer, which removes the elongated molecule. Because of the mass removal, the frequency reverts back to phase one, as does the dissipation because the surface is going back to rigid film.

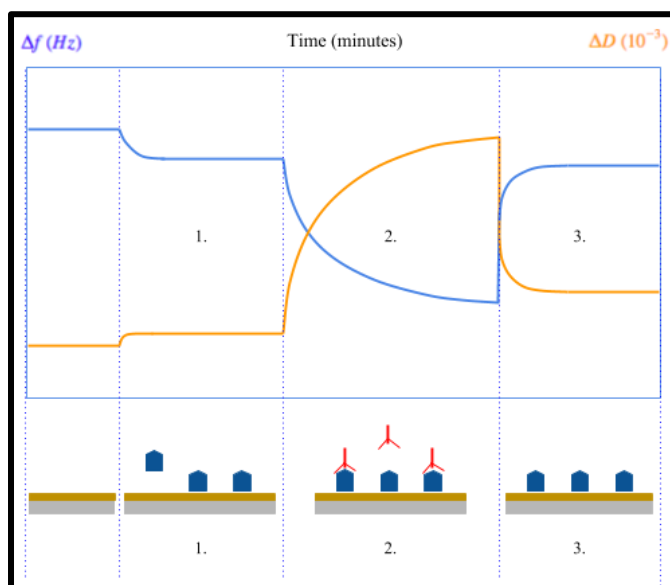


Figure 3. A schematic outlining the change in frequency (blue) and dissipation (orange) throughout the process of adding and removing an elongated molecule to a rigid surface. This schematic has been adapted from a concept of Q-Sense Technologies.

In Figure 3, mass changes correlate to a change in frequency, and any structural property changes result in a change in dissipation. The quartz crystal from the QCM-D oscillates as its resonance frequency. As the mass changes at the surface, changes in frequency are measured; when molecules absorb into the surface, the frequency decreases. With these oscillations, the dissipation (which is damping) are shown as well. As explained for Figure 3, a formation of a soft molecular layer increases the dissipation. Dissipation is low with a rigid surface. Figure 4 shows the correlation between a rigid surface, versus a soft surface as it correlates to frequency and dissipation. The red shows the oscillations with a rigid surface, while the oscillations in green explain the soft surface.

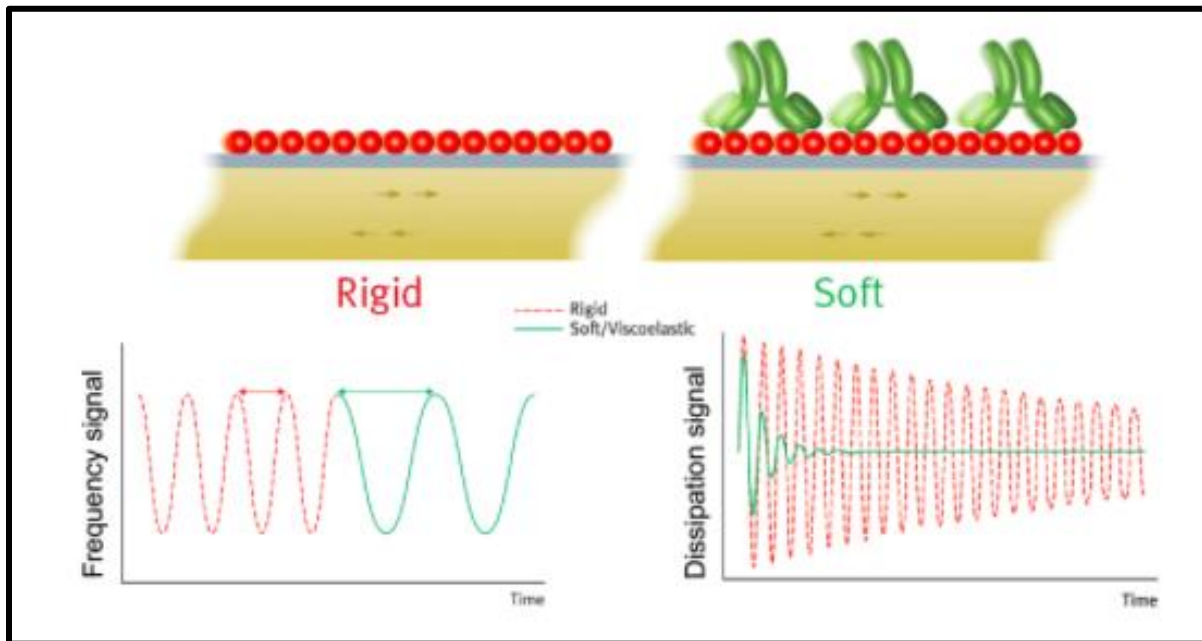


Figure 4. The frequency and dissipation oscillations as a function of time, considering a rigid surface (in red) and a soft surface (in green) (“Q-Sense Technologies”).

Because the QSense Analyzer can measure so many parameters at once, it often is able to compute the mass, thickness, and concentrations within one trial. In order to ensure that the product is producing accurate results, it is considered that we can calculate an estimated mass (m) of the adhering layer using the Sauerbrey relation:

$$\Delta m = - \frac{C * \Delta f}{n}$$

Equation 1. The Sauerbrey Relation

In this equation, C is equal to $17.7 \text{ ng Hz}^{-1} \text{ cm}^{-2}$ for a 5 MHz quartz crystal, and n is the overtone number, which can be 1, 3, 5, or 7. Additionally it is possible to estimate the thickness (d) of the adhering layer, where ρ_{eff} is the effective density of the adhering layer:

$$d_{\text{eff}} = \frac{\Delta m}{\rho_{\text{eff}}}$$

Equation 2. Thickness Estimate

These equations act as a form of confirmation that the QCM-D is reading and analyzing the data properly, thus producing the results needed by the equipment.

2.5. Replication of Environmental Conditions: Humic Substances as NOM Analogs

Engineered nanoparticles (ENP) enter the environment from industrial sources and interact with chemicals in the ecosystem to produce toxic effects. Since NP behavior in the ecosystem is dependent on the conditions of the chemistry (primarily pH, temperature, and complex formation), SLB studies aiming to replicate environmental conditions must consider silver NP interaction with natural organic matter (NOM). Our experiments use humic substances to replicate the matrix formed by silver NPs and NOM in the environment.

2.6. Natural Organic Matter (NOM)

Natural organic matter (NOM) is a complex matrix present in soil, peat, coal and water around the world. NOM forms via the decomposition of plant and animal material and, as the product of the particular organisms from an ecosystem, varies widely in structure and properties. NOM acts as a stabilizer for ENPs in aqueous solutions while increasing the surface area to volume ratio of the particle. The increased surface area and reduced volume of the structure expands the chemical reactivity of the ENP thereby exacerbating its toxicological effects in the environment. Recent studies have demonstrated that the aggregation rate of silver NPs (coated with citrate) increased with increasing ionic strength and decreasing NOM concentration (Bae, 2013). The aggregation behavior of NOM therefore dominates the deposition and dissolution of NPs. Microbial toxicity of zinc oxide (ZnO) NPs was reduced in the presence of dissolved organic matter (DOM) due to a stereochemical decrease in direct membrane interaction (Aiken, 2011).

The complexity of the matrix makes characterizing the NOM at the molecular level difficult, but recent techniques using spectroscopic methods as well as chemical and thermal degradation have elucidated key structural components (Derenne, 2014). Typically, NOM contains one hydrophobic and one hydrophilic region. The hydrophobic region of the matrix is comprised of carbon and nitrogen in the form of carboxylic and tannic acids in addition to an assortment of proteins. The hydrophilic structural component is called a humic substance and consists of aromatic carbons with conjugated double bonds.

2.7. Humic Substances as NOM Replicates

The simulation of silver NP complexes in the environment are important for understanding the effects of agglomeration on particle transport and toxicity. Humic substances are heterogeneous by-products of microbial metabolism and that provide the familiar properties of soil: mobilization and sequestration (Sutton, 2005). Recent characterization techniques have revealed that the mechanism of humic substance agglomeration in solution is supramolecular association in which various organic molecules become chemically linked via hydrogen bonds and hydrophobic forces (Sutton, 2005).

Humic substances, which we use in place of NOM, are categorized according to their solubility at different pH conditions. Humic acids (HA) comprise the fraction that is insoluble at low pH whereas fulvic acids (FA) are low molecular weight compounds that are soluble over a wide pH range (Reidy, 2013). HA have higher hydrophobicity and less negative charge than FA making them more susceptible to aggregation disruption in the presence of organic materials with both hydrophobic and hydrophilic segments (Sutton, 2005).

The exact properties and structure of a given sample of humic substance varies according to the water or soil source and the method of extraction. We therefore incorporated five different types of humic substances into our experimental design: four HA of an array of molecular weights and one FA. Aldrich humic acid (AHA) of 50,000 Da and 20,000 Da provide high molecular weight agglomeration solutions while Suwannee River humic acid (SRHA) (1,100 Da) and Suwannee River fulvic acid (SRFA) (700 Da) control for the source of humic substances. Elliot soil humic acid (ESHA) with a molecular weight of 12,700 Da provides an alternative HA source separate from Suwannee River.

The Suwannee River samples were obtained by the International Humic Substances Society (IHSS) at the Okefenokee Swamp in Georgia. The source of the dissolved organic carbon (DOC) in the Suwannee River substances is primarily vegetation from the swamp with levels typically below 75 mg/L. The Elliott Soil samples were also collected and processed by the IHSS from the grassland soils of Indiana, Illinois, and Iowa (“Source Materials for IHSS Samples” 2017). The ESHA derive from poorly-drained soils of silty material. According to the IHSS, each sample must meet the following standards:

1. The sample must have come from a site specifically designated by the IHSS.
2. The sample must have been prepared according to a specific procedure designated by the IHSS.
3. The operations involved in (1) and (2) must have been conducted under the direct supervision of the IHSS.
4. The sample must be designated as a standard by the IHSS.

The IHSS collection strategy controls for variations in sample properties that would result from using a variety of geographical sources and different isolation protocols. Further, the consistency of the humic substance source enables comparisons of NOM properties, and thus NP-complex activity, across experiments.

2.8. Hypothesis

Based on our literature review and background research, it is expected that the lower molecular weight NOM analogs (SRHA and SRFA) will induce more severe bilayer disruptions than the higher molecular weight samples (ESHA and LHAS) across each NP size.

3. Methods and Materials

3.1. Silver Nanoparticles

Spherical, silver nanoparticles with diameters of 5, 20, and 50 nm were purchased (Nanocs, Inc.; New York, NY). The size distribution (15%) of the stock solutions purchased from Nanocs were confirmed using dynamic light scattering and the Zeta potentials were determined using a Malvern Zetasizer at the purchased concentration. The silver NPs were diluted from a manufactured stock concentration of 10^{14} particles/mL to an experimental concentration of 1×10^{10} particles/mL. The NP solutions were stored at 7 °C in a light-blocking container and were diluted with ultrapure water (Milli Q) before experimentation.

3.2. Humic Substances

Suwannee River Fulvic Acid Standard II (SRFA), Suwannee River Humic Acid Standard II (SRHA), Elliott Soil Humic Acid Standard IV (ESHA), and Leonardite Humic Acid Standard—100 mg each—were purchased, in powder form, from the International Humic Substances Society (IHSS). Humic stock solutions of 200 mg/L were prepared by adding the powder to ultrapure water (Milli Q), stirring for 1 hour at 30 °C, and sonicating the solution for 1 hour in a water bath ultrasonicator. The humic solutions were stored at 7 °C in a light-blocking container and were re-agitated for one hour and filtered twice—using a 0.2 µm syringe filter—before experimentation. Humic substance concentration was controlled at 20 mg/L for all experiments.

The solution and aggregation properties (pH, size distribution, and polydispersity) of the humic substances were measured in aqueous solution alone (without buffer) and in the presence of NPs (at both the low and high experimental concentrations without buffer). The pH was measured and a 1 mL sample was transferred to a cuvette; DLS readings were taken at 1 minute intervals for 10 minutes. The 10-minute period for DLS measurements was chosen to parallel the 10 minute flow protocol for our QCM-D experiments. To measure the aggregation of the humic substances in the presence of silver NPs at the lower experimental concentration of 2×10^{12} particles/mL, a 50 mL solution was prepared consisting of 25 mL of 200 mg/L humic stock solution, 1 mL of silver NP stock (10^{14} particles/mL), and 24 mL of water. The pH was measured and a 1 mL sample was transferred to a cuvette for DLS measurements.

3.3 Vesicle Preparation

L- α -phosphatidylcholine (egg, chicken) (PC) with purity of greater than 99% was purchased from Avanti Polar Lipids. Lipid vesicles were prepared according to an established laboratory protocols in which 15 mg of egg PC (stocked in ethanol at 100 mg/mL) was dried in a test tube under a steady nitrogen gas stream and allowed to desiccate for 24 hours. The dried PC solution—now existing as a film adhered to the inner surface of the tube—was then rehydrated in 6 mL of a buffer solution containing 10 mM HEPES 4-(2-hydroxyethyl)-1-piperazineethanesulfonic acid and 100 mM sodium chloride at pH 7.0 ± 0.05 . The solution (now at a PC concentration of 2.5 mg/mL) then entered the freeze-thaw-vortex cycle where it underwent 5 rotations of freezing in the presence of dry ice (approximately 10 minutes), thawing in a 30° C water bath (approximately 5 minutes), and vortexing on the highest setting (30

seconds). An ultrasonic dismembrator (Model 150T, Fisher Scientific, Waltham, MA) was used to form small unilamellar lipid vesicles (<100 nm in diameter) by sonicating the PC solution in an ice bath for 30 minutes in pulse mode at a 30% duty cycle (3-second pulse on, 7-second pulse off) and an amplitude of 60. To remove titanium residue from the vesicle solution following sonication, the PC was centrifuged in an Eppendorf Centrifuge 5415 D at 16000 rcf for 10 minutes. The supernatant was then separated from the titanium accumulated at the bottom of the Eppendorf vial and stored under nitrogen gas at 7°C. The average vesicle size was determined to be 75 nm as measured by dynamic light scattering (Malvern Zetasizer). The 2.5 mg/mL stock vesicle suspension was diluted to 0.1 mg/mL using HEPES–NaCl buffer before experimentation.

3.4. Quartz Crystal Microbalance with Dissipation (QCM-D) Monitoring for Nanoparticle Interaction with Supported Lipid Bilayers

A Q-Sense E4 (Biolin Scientific, Sweden) was used to record QCM-D measurements on silicon dioxide sensor crystals (Gothenburg, Sweden). Frequency and dissipation measurements for overtones 3, 5, 7, 9, and 11 of the sensor crystal's natural frequency of 5 MHz were normalized by the Q-Sense software prior to beginning each experiment. These overtones correspond to bilayer depth; overtone 3 relates frequency and dissipation changes near the bilayer surface while overtone 11 applies to the hydrodynamic layers adjacent to the silica substrate. Before each experiment, the crystals were cleaned using a modification of the Q-Sense protocol in which ethanol, ultrapure water, 2% sodium dodecyl sulfate, and ultrapure water were flown through the chambers sequentially for 5 minutes. Once the crystals were dried under a gentle nitrogen stream, they were treated with two 45-second cycles of oxygen plasma etching (Plasma Prep II; SPI Supplies, West Chester, PA) to remove any remaining organic contaminants.

Measurement baselines were recorded for the sensors in both air and liquid (after introduction of buffer to chamber) before forming the supported lipid bilayer on the crystal surface. The PC vesicles, diluted from a stock concentration of 2.5 mg/mL to an experimental concentration of 0.1 mg/mL, were flowed over the sensors at 0.15 mL/min until a stable bilayer was formed (approximately 5 minutes). The PC bilayer on the sensor surface was rinsed with HEPES buffer solution for 5 minutes before introducing a 5 minute ultrapure water flow to the system to compensate for the viscosity difference between buffer and water. The NP solution (including applicable humic substances) was then flown for 10 minutes before the bilayer was rinsed with HEPES buffer for 5 minutes. Experiments were performed with NPs alone and with NPs in the presence of humic substances, controlling for humic substance concentration (100 mg/L in all experiments) and NP concentration (2×10^{12} and 8×10^{12} particles/mL for the low- and high-concentration experiments respectively). Modeling and analysis of the QCM-D data was performed using QTools software.

4. Results

4.1. Characterization of Humic Substances

The humic substances were characterized by focusing on their tested pH values and their molecular weights. Table 1 shows an outline of the different values for each humic substance. The pH values were recorded to quantify the viscoelastic changes that resulted from deviations from the ultrapure water baseline. When dissolved in DI water, the humic acids generally produced pH values less than 3, while the fulvic acid had the lowest measured pH, as expected.

Table 1. A description of the pH and molecular weight of each tested humic substances.

NOM Analog	Aqueous Solution pH (200 mg/L)	Molecular Weight (Da)
Suwannee River Humic Acid Standard II (SRHA)	2.98	1,100
Suwannee River Fulvic Acid Standard II (SRFA)	3.45	700
Elliott Soil Humic Acid Standard IV (ESHA)	2.75	12,700
Leonardite Humic Acid Standard (LHAS)	3.41	18,000

4.2. SLB Formation by QCM-D

The QCM-D response of frequency and dissipation changes in each experiment involving the silver NPs are summed up by using two graphs in Figure 5. Figure 5 shows an example of the frequency and dissipation changes for the test solution containing 1×10^{10} 20 nm silver NP/mL control (A) and the changes for the test solution containing 20 mg/L SRHA equilibrated with 1×10^{10} 20 nm silver NP/mL (B). The blue toned colors represent the frequency changes, while the orange toned colors represent the dissipation changes. At the start of the recorded data, a stable lipid bilayer was formed and the bilayer formation began to be recorded by the QCM-D in different stages. In Stage 1, there is a clear decrease in frequency due to the increase in mass observed by vesicle fusion to the quartz crystal surface. A soft film formation is indicated in Stage 1 by the dissipation increase. At the beginning of Stage 2, the Tris buffer is added which causes a shift in the frequency and dissipation of both experiments, which is more visible when looking at the dissipation changes. Since about halfway through Stage 1, the frequency values begin increasing again due to the molecules absorption into the surface, because of the buffer flow that removed any of the un-ruptured vesicles. The vesicles rupture spontaneously and form the supported lipid bilayer. The dissipation changes are seen due to the added mass which then softened the film. Beginning in Stage 3, the water rinse begins in order to prepare the solution for the nanoparticle contact in the next stage. The addition of water increases the mass change

(which increases the frequency), further softening the film and reverting back to the initial interactions the QCM-D measured before the mass was observed. This occurs because of the slightly lower viscosity and density of the water than was previously introduced from the Tris buffer solution. In (A) of Figure 5, there is no noticeable change from Stage 3 until Stage 5. The addition of just silver NP without humic substances showed no clear change. Part (B) of Figure 5 shows a small, but visible difference in frequency and dissipation in Stage 4. This is when the test solution was added of the silver NP with SRHA for 10 minutes. At this point, the frequency slightly decreased indicating mass change at the introduction of the test solution, as did the dissipation and rigidity of the film. The small changes, however, indicated that there may not have been a large effect of the test solution on the humic substance. Through Stage 5, water was flowed through the QCM-D to rinse for 10 minutes. Similar trends were found throughout each similar experiment. That is, each control showed similar trends as the control experiment shown below, and each experiment with humic substances equilibrated with silver nanoparticles showed similar trends as shown in part (B) of the figure.

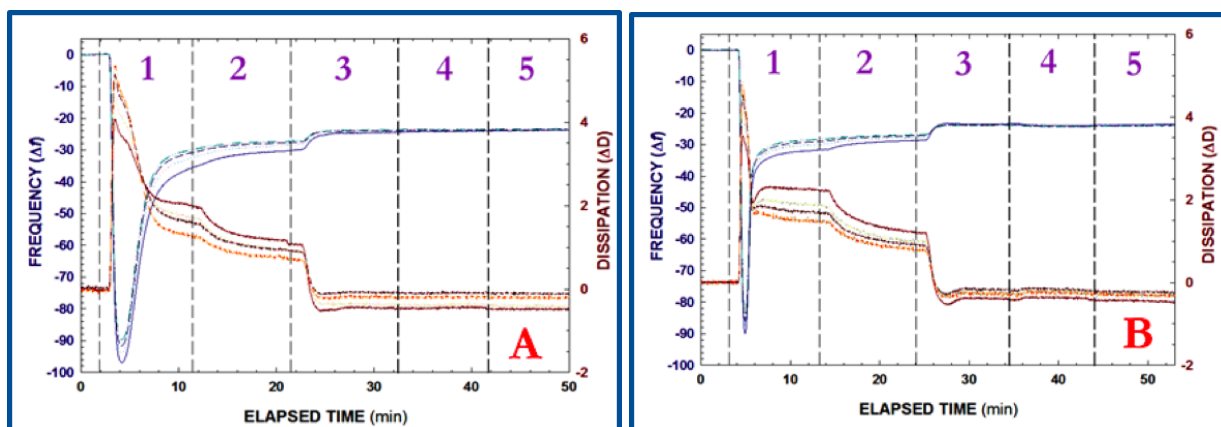


Figure 5. The frequency and dissipation changes for test solution (introduced in Stage 4) containing (A) 1×10^{10} 20 nm silver NP/mL control and (B) 20 mg/L SRHA equilibrated with 1×10^{10} 20 nm silver NP/mL

4.3. Interaction of SLB with NPs in the Presence of Humic Substances

To characterize the frequency and dissipation changes caused by the interaction of the test solution with the SLB, we developed ΔF and ΔD bar charts. The ΔF and ΔD bar charts depict the scaled changes in frequency and dissipation between a point in time before the introduction of the test solution and after the 10 minutes of test solution flow. For our data analysis, we chose the initial time point of two minutes before the end of ultrapure water flow in stage 3 and the final time point of eight minutes into the water rinse of stage 5. Ideally, this systematic approach to extracting the frequency and dissipation changes isolates the effect of the test solution on the SLB.

Each bar chart reflects the averages of four experimental replicates across overtones 3 through 11, corresponding to the aforementioned depths of the film (in our case a PC bilayer). To obtain the frequency and dissipation changes depicted in the plots, the initial time point value for each overtone of each chamber was subtracted from its final time point value and averaged between like replicates. In this manner, negative changes in frequency represent an increase in mass on the crystal, while positive changes in frequency indicate a decrease in crystal mass.

Dissipation changes, which relay the evolution of the film's viscoelasticity, were minor for each test solution outside of the SRHA control and the SRHA equilibrated with 40 nm NP.

Figure 6 depicts the frequency and dissipation changes for the NP controls of each size tested (the test solutions containing 20, 40, and 50 nm NP without humic substances present).

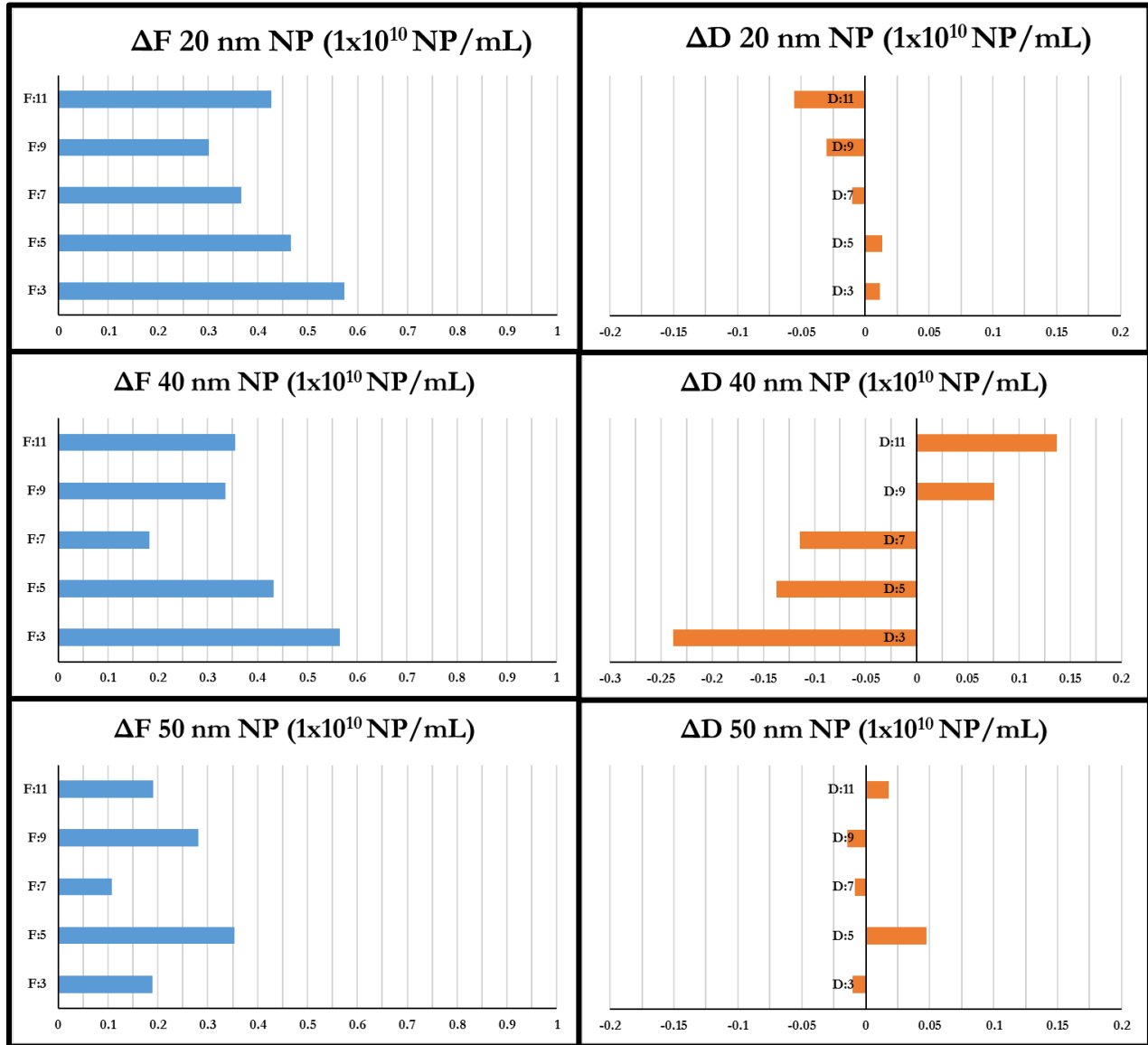


Figure 6. The ΔF and ΔD bar charts for the 20, 40, and 50 nm NP control solutions.

Figure 7 depicts the frequency and dissipation changes for the humic substance controls (those test solutions containing SRHA, ESHA, SRFA, and LHAS exclusively, without NPs).

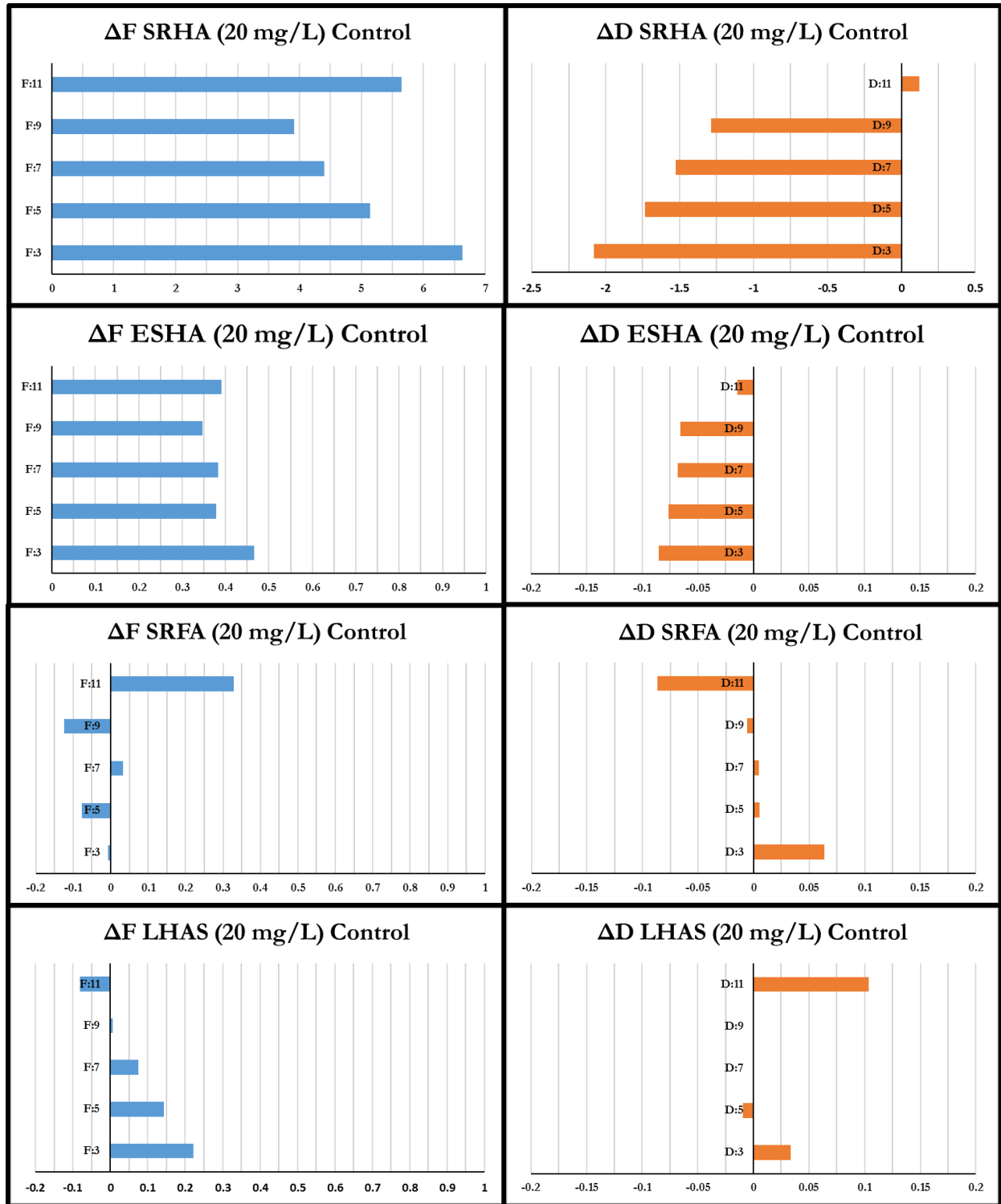


Figure 7. The ΔF and ΔD bar charts for humic substance control solutions.

Figure 8 depicts the frequency and dissipation changes for the 20 nm NP solutions equilibrated with each of the four tested NOM simulants (SRHA, ESHA, SRFA, and LHAS).

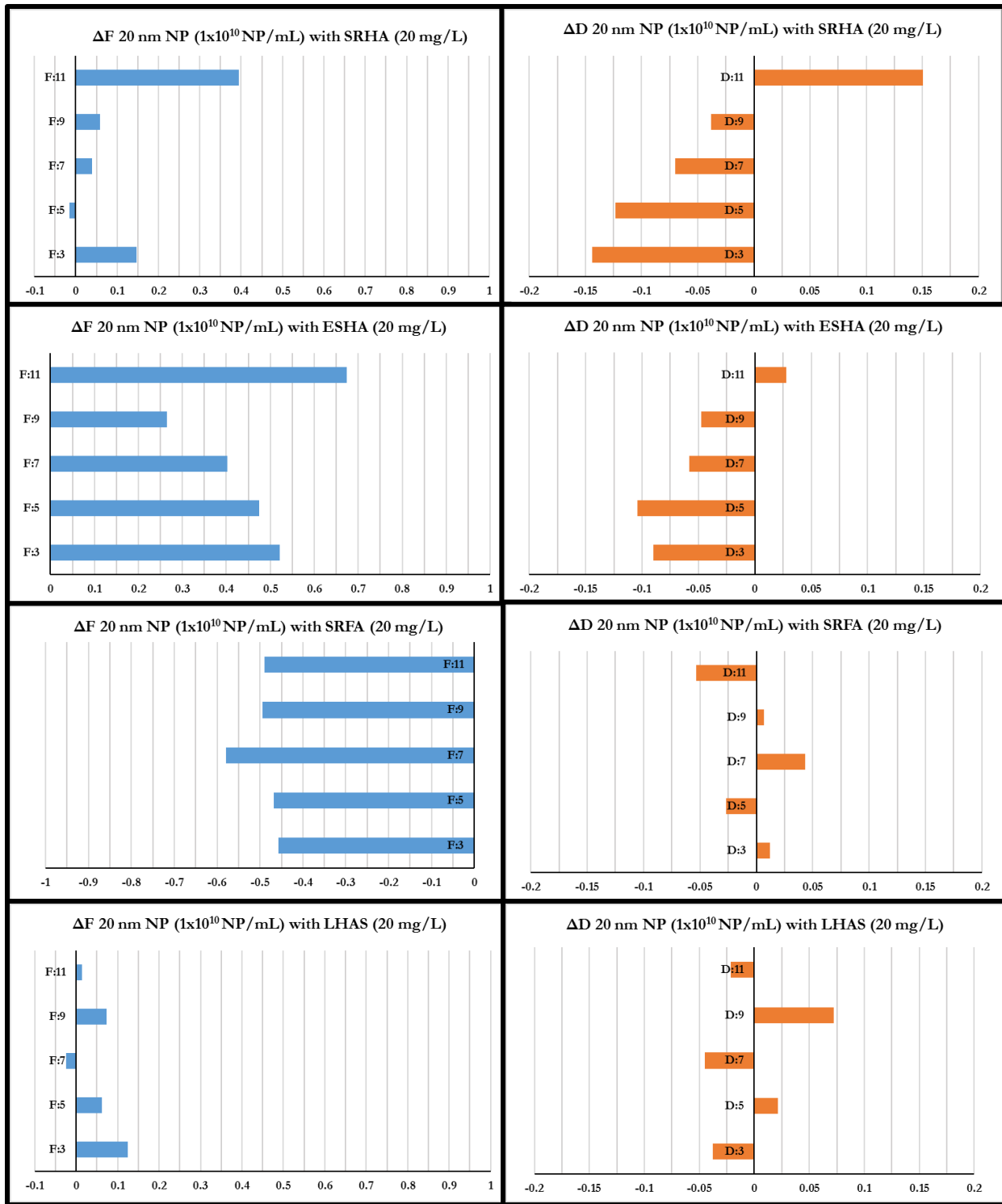


Figure 8. The ΔF and ΔD bar charts for the 20 nm NPs equilibrated with SRHA, ESHA, SRFA, and LHAS.

Figure 9 depicts the frequency and dissipation changes for the 40 nm NP solutions equilibrated with each of the four tested NOM analogs (SRHA, ESHA, SRFA, and LHAS).

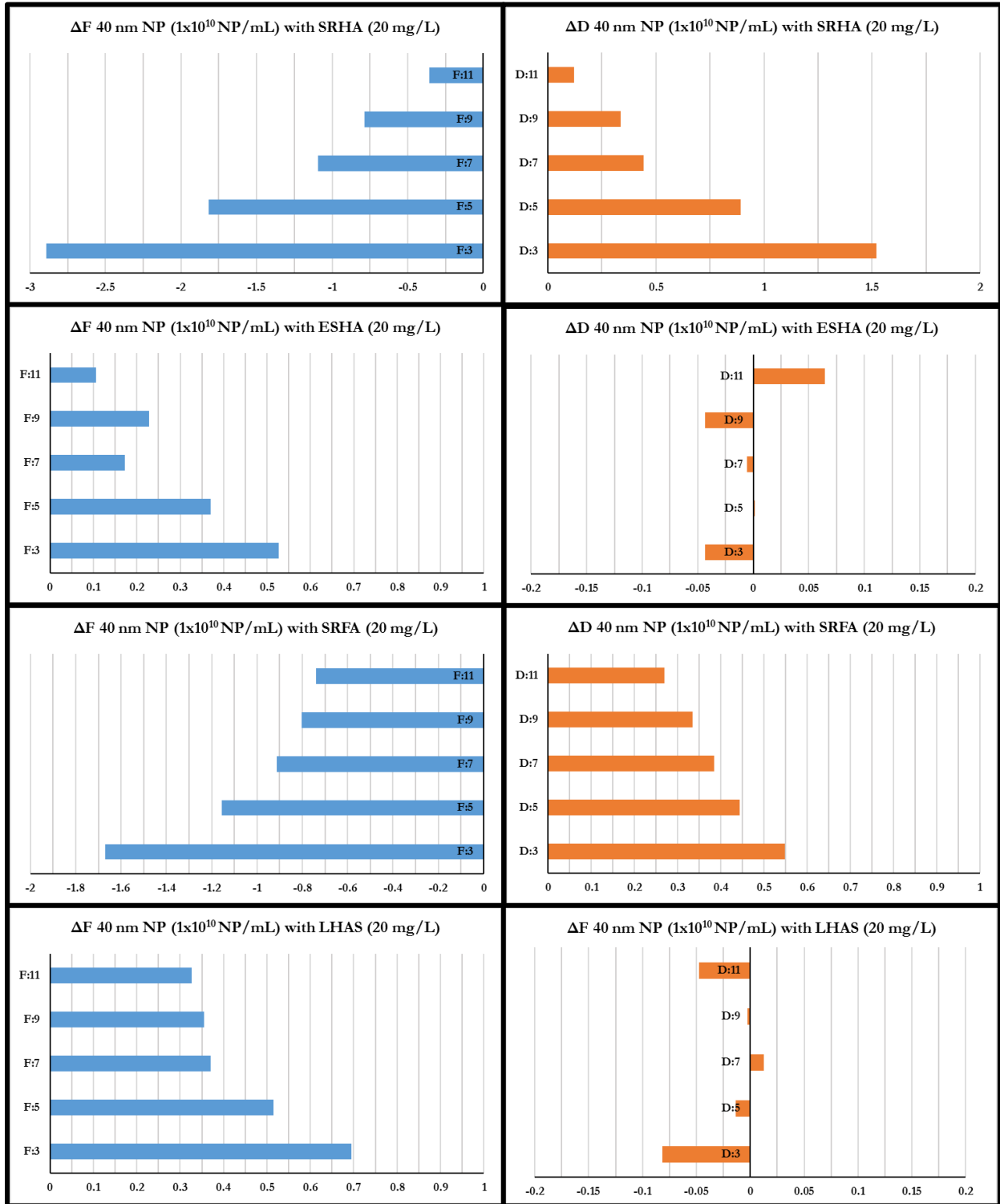


Figure 9. The ΔF and ΔD bar charts for the 40 nm NPs equilibrated with SRHA, ESHA, SRFA, and LHAS.

Figure 10 depicts the frequency and dissipation changes for the 50 nm NP solutions equilibrated with each of the four tested NOM simulants (SRHA, ESHA, SRFA, and LHAS).

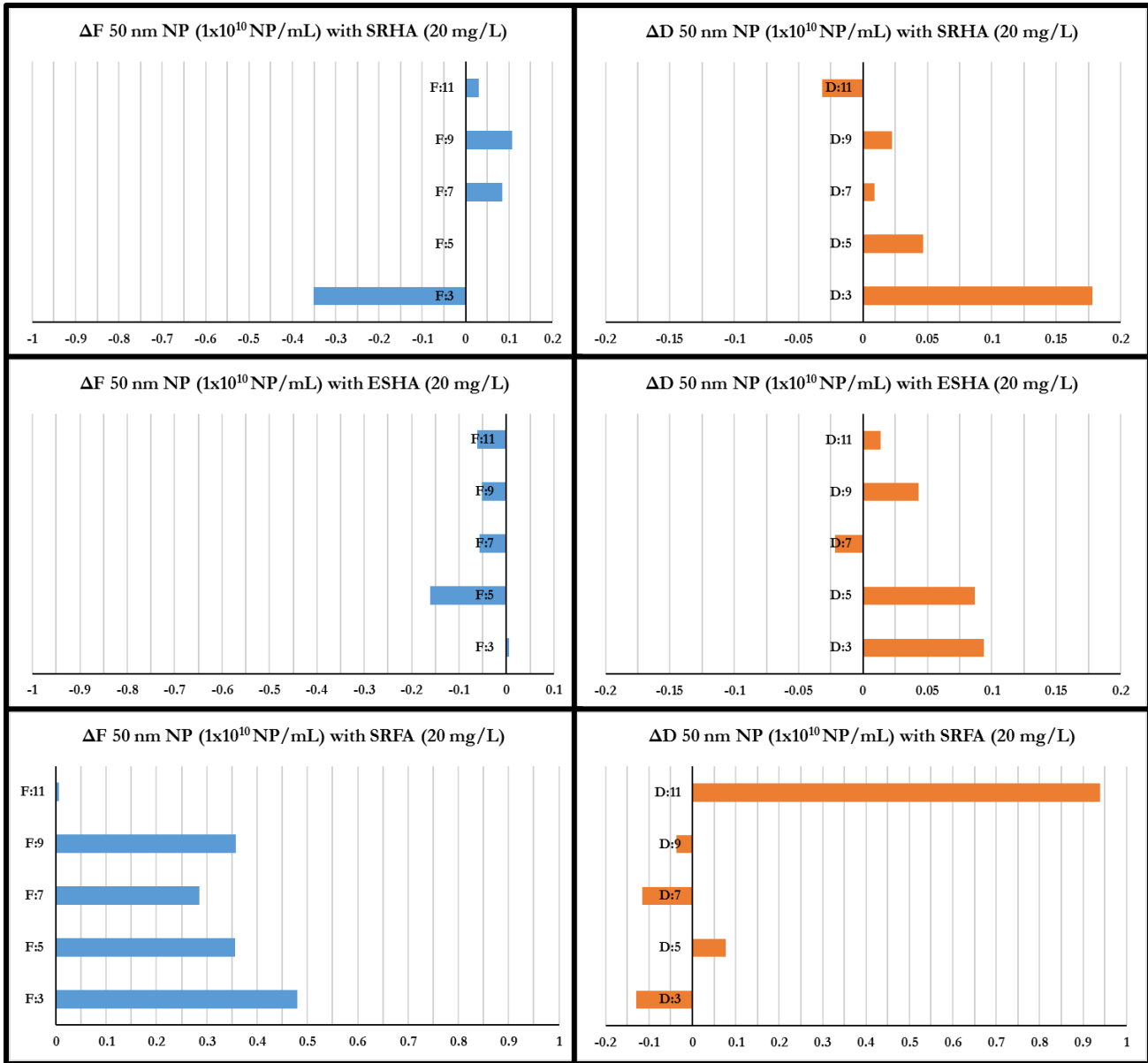


Figure 10. The ΔF and ΔD bar charts for the 40 nm NPs equilibrated with SRHA, ESHA, SRFA, and LHAS.

5. Discussion

5.1. SRHA Induced the Only Significant SLB Disruption

For an SLB interaction to be considered significant, we expected the frequency change to be greater than one Hertz. A one Hertz change is approximately a 17.6 ng/cm^2 change in mass. Any frequency value collected that remained under one Hertz was assumed to be noise, with no significant bilayer disruption. It was expected to see a significant amount of mass change with all test solutions, but instead bilayer destabilization was only observed among the test solutions containing SRHA. Even so, disruption only emerged from the SRHA control and the SRHA equilibrated with 40 nm NP. The greatest frequency change of 6.5 Hertz, totaling a mass change of 114.4 ng/cm^2 , was observed by the SRHA control test solution which did not contain NP. The positive frequency change indicated a decrease in mass. The observed mass decrease resulted from the uptake of lipid molecules from the bilayer. Interestingly, the removal of lipids from the bilayer was not limited to surface interactions but rather occurred relatively uniformly across each overtone. This result was more than twice the next largest frequency change, 2.75 Hz, observed by the test solution containing SRHA equilibrated with 40 nm NP nanoparticles. However, the negative change in frequency induced by the equilibrated solution indicated mass was deposited on the bilayer surface. This could be explained by SRHA functionalization in the presence of NP, although the absence of similar results among the SRHA equilibrated solutions of other sizes suggests that this observation may be an outlier.

5.2. Humic Substance Molecular Weight Did Not Affect Disruption Mechanics

It was expected that lower density NOM analogs, SRHA and SRFA, would induce more severe bilayer interaction than the more dense simulants, ESHA and LHAS. However, since the only test solutions containing SRHA produced significant interaction profiles, the molecular weight of the humic substance appears to have no significance on bilayer disruption at these concentrations. Further, the absence of observed frequency changes in the SRHA test solutions containing 20 nm and 50 nm NP, in conjunction with the opposing mechanisms of action among the two test solutions in which mass changes occurred (the control solution showed mass decrease whereas the 40 nm solution demonstrated mass increase), hedges the significance of the SRHA conclusions. Thus, the non-uniform results for the SRHA solutions demands additional testing to ensure repeatability beyond four replicates.

5.3. Recommendations for Future QCM-D Analysis of NP-Induced SLB Disruption in the Presence of NOM

If there were a higher concentration of nanoparticles, more severe disruptions might have been observed. Our chosen NP concentration of 1×10^{10} was restricted by the highest NP concentration that could be achieved given NP stock concentrations of the same molar concentration, 0.1 M Ag, at different sizes (the 50nm NP stock was significantly less concentrated in units of particles/mL). A different size of nanoparticles also might have induced more significant results, since smaller or larger NP may be more or less susceptible to functionalization in the presence of humic substances. Since the effect on the bilayer relies heavily on the molecular properties of the humic substance, the differences in behavior of

equilibrated solutions containing silver and gold nanoparticles are likely different. Therefore, the chosen NOM concentration of 20 mg/L (which was picked to mirror environmental conditions and kept constant throughout each experiment) may be too low for observable frequency changes at the given conditions. Since a disparity has emerged between the observed frequency changes at NOM concentrations of 100 mg/L and 20 mg/L, it is vital for future research to explore the relationship between humic substance concentration and bilayer destabilization.

6. Conclusion

The purpose of this investigation was to explore the effect of engineered silver nanoparticle sizes on bilayer disruption in the presence of humic substances. Since NOM has been observed to act as a stabilizing agent for nanoparticles that increases their toxicological effects, we expected our project to reveal similar trends. We used QCM-D to isolate the effect of NP and NOM test solutions on single-component PC SLBs across three silver nanoparticle sizes: 20 nm, 40 nm, and 50 nm. We tested NP solutions equilibrated with four humic substances: Suwannee River Humic Acid Standard II (SRHA), Suwannee River Fulvic Acid Standard II (SRFA), Elliott Soil Humic Acid Standard IV (ESHA) and Leonardite Humic Acid Standard (LHAS). The lower molecular weight NOM analogs (SRHA and SRFA) did not induce more significant bilayer disruptions than their high-molecular weight counterparts (ESHA and LHAS). Based on the changes in frequency and dissipation observed across the time of test solution flow (which isolated the effect of the test solution on the SLB), only SRHA produced any significant perturbations. Further, the disruption produced by SRHA was exclusively observed in the control test (in which frequency changes were most severe) and 40 nm NP equilibrated solutions. The absence of bilayer disruption in the other test groups indicated that either the tested NP concentration of 1×10^{10} particles/mL or NOM concentration of 20 mg/L were below the threshold for observable destabilization. Therefore, further research is recommended to explore the effect of NP and humic substance concentration on SLB disruption.

References

Aiken, George R., Hsu-Kim, Heileen and Joseph N. Ryan. "Influence of Dissolved Organic Matter on the Environmental Fate of Metals, Nanoparticles, and Colloids." (2011). *Environmental Science & Technology*. 45 (8), pp. 3196-3201. DOI: 10.1021/es103992s

Bae S, Hwang YS, Lee Y-J, Lee S-K. "Effects of Water Chemistry on Aggregation and Soil Adsorption of Silver Nanoparticles." *Environmental Health and Toxicology*. (2013) 28:e2013006. doi:10.5620/eht.2013.28.e2013006.

Bailey, C., Kamaloo, E., Waterman, K., Wang, K., Nagarajan, R. and Camesano, T. (2015). "Size dependence of gold nanoparticle interactions with a supported lipid bilayer: A QCM-D study." *Biophysical Chemistry*, 203-204, pp.51-61.

Bailey, Regina. "Cell Membrane Function and Structure." ThoughtCo. October 9th, 2017 2017. Web. <<https://www.thoughtco.com/cell-membrane-373364>>.

Castellana, Edward, and Paul Cremer. "Solid Supported Lipid Bilayers: From Biophysical Studies to Sensor Design." *Science Direct* 61.10 (2006): 429-44. Print.

Cooper GM. "The Cell: A Molecular Approach." 2nd edition. Sunderland (MA): Sinauer Associates; 2000. Cell Membranes. Available from: Web.<https://www.ncbi.nlm.nih.gov/books/NBK9928/>.

Derenne, Sylvie, Tu, Thanh Thuy Nguyen. "Characterizing the molecular structure of organic matter from natural environments: An analytical challenge." *Comptes Rendus Geoscience*. (2014) 346(3-4). pp 53-63, ISSN 1631-0713, <https://doi.org/10.1016/j.crte.2014.02.005>.

H. Heerklotz and J. Seelig. "Leakage and lysis of lipid membranes induced by the lipopeptide surfactin." *European Biophysics Journal* (2007) 36, pp. 305–314.

"Minimize Downtime and Maximize Seal Performance with Viton™ Fluoroelastomers." The Chemours Company. (2017) www.chemours.com/Viton/en_US/.

Mulvihill, Marty, and Wendy Hessler. "Silver from Nanoparticles Found in Plants and Animals." *Silver from Nanoparticles Found in Plants and Animals. Environmental Health News*, 15 June 2012.

Kamaloo, Elaheh, et al. "Effect of Concentration on the Interactions of Gold Nanoparticles with Model Cell Membranes: A QCM-D Study." *Nanotechnology to Aid Chemical and Biological Defense NATO Science for Peace and Security Series A: Chemistry and Biology*, 2015, pp. 67–76., doi:10.1007/978-94-017-7218-1_5.

“Nanosilver: Environmental Effects.” Beyond Pesticides, Protecting Health and the Environment, beyondpesticides.org/programs/antibacterials/nanosilver/environmental-effects.

Reidy, B., Haase, A., Luch, A., Dawson, K. A., & Lynch, I. “Mechanisms of silver nanoparticle release, transformation and toxicity: a critical review of current knowledge and recommendations for future studies and applications.” *Materials*. (2013) 6(6). Pp.2295-2350.

Ritcher, Ralf, Remi Beret, and Alain Brisson. "Formation of Solid-Supported Lipid Bilayers: An Integrated View." *American Chemical Society* 22.8 (2006): 3497-505. Print.

“Source Materials for IHSS Samples.” International Humic Substance Society (IHSS). (2017).

Sutton, Rebecca and Sposito, Garrison. “Molecular Structure in Soil Humic Substances: The New View.” *Environmental Science & Technology*. (2005) 39 (23). pp. 9009-9015. DOI: 10.1021/es050778q

“Q-Sense Technologies.” Biolin Scientific, www.biolinscientific.com/q-sense/technologies/.

Welles, Audrey E.. *Silver Nanoparticles: Properties, Characterization and Applications*, Nova Science Publishers, Inc., 2010. ProQuest Ebook Central, <https://ebookcentral-proquest-com.ezproxy.wpi.edu/lib/wpi/detail.action?docID=3018056>.

World, James Urquhart.. “Silver Nanoparticles in Clothing Pose No New Risk.” *Scientific American*, 15 July 2014, www.scientificamerican.com/article/silver-nanoparticles-in-clothing-pose-no-new-risk/.